



# P-glycoprotein (ABCB1/MDR1) limits brain accumulation and Cytochrome P450-3A (CYP3A) restricts oral availability of the novel FGFR4 inhibitor fisogatinib (BLU-554)

Wenlong Li<sup>a</sup>, Rolf Sparidans<sup>b</sup>, Mujtaba El-lari<sup>a</sup>, Yaogeng Wang<sup>a</sup>, Maria C. Lebre<sup>a</sup>,  
Jos H. Beijnen<sup>a,b,c</sup>, Alfred H. Schinkel<sup>a,\*</sup>

<sup>a</sup> Division of Pharmacology, The Netherlands Cancer Institute, Plesmanlaan 121, 1066 CX Amsterdam, the Netherlands

<sup>b</sup> Faculty of Science, Department of Pharmaceutical Sciences, Division of Pharmacology, Utrecht University, Universiteitsweg 99, 3584 CG Utrecht, the Netherlands

<sup>c</sup> Department of Pharmacy & Pharmacology, The Netherlands Cancer Institute, Plesmanlaan 121, 1066 CX Amsterdam, the Netherlands

## ARTICLE INFO

### Keywords:

Fisogatinib (BLU-554)  
Fibroblast growth factor receptor 4  
P-glycoprotein  
Brain accumulation  
Cytochrome P450-3A  
Oral availability  
Oatp1a/1b

## ABSTRACT

Fisogatinib (BLU-554) is a highly selective and potent oral fibroblast growth factor receptor 4 (FGFR4) inhibitor currently in Phase I clinical trials for treatment of hepatocellular carcinoma (HCC). Using (male) genetically modified mouse models, we investigated the roles of the multidrug efflux transporters ABCB1 and ABCG2, the OATP1A/1B uptake transporters, and the drug-metabolizing CYP3A complex in fisogatinib pharmacokinetics. *In vitro*, fisogatinib was modestly transported by hABCB1. Upon oral administration of 10 mg/kg fisogatinib, its brain accumulation was substantially increased in *Abcb1a/1b*<sup>-/-</sup> (6.3-fold) and *Abcb1a/1b;Abcg2*<sup>-/-</sup> mice (7.2-fold) compared to wild-type mice, but not in single *Abcg2*<sup>-/-</sup> mice. The oral plasma pharmacokinetics and liver distribution of fisogatinib were not significantly affected by the absence of Oatp1a/1b drug uptake transporters. We further found that plasma exposure of fisogatinib in *Cyp3a*<sup>-/-</sup> mice increased by 1.4-fold, and was subsequently 1.6-fold decreased upon transgenic overexpression of human CYP3A4 in liver and intestine. However, the relative tissue distribution of fisogatinib remained unaltered. In summary, in mice, fisogatinib brain accumulation is substantially limited by ABCB1 P-glycoprotein in the blood-brain barrier, and oral availability of fisogatinib is markedly restricted by CYP3A activity. The obtained insights may be useful for optimizing the clinical efficacy and safety of fisogatinib.

## 1. Introduction

Cancer is the second leading cause of death in the world, accounting for an estimated 9.6 million deaths in 2018 (Bray et al., 2018). Liver cancer is one of the most common causes of cancer-related deaths (Bray et al., 2018). The leading cause of liver cancer is cirrhosis due to alcohol abuse, hepatitis (B or C) viral infection and/or exposure to carcinogenic substances (like cigarettes, herbicides, or dietary fungal toxins) (Balogh et al., 2016).

The most common primary malignant cancer of the liver is

hepatocellular carcinoma (HCC), which makes up 80% of cases (Balogh et al., 2016). HCC is refractory to conventional chemotherapy, and there has been minimal progress for the treatment of this disease in the past 20 years. The multikinase inhibitors sorafenib and regorafenib have been approved recently for the treatment of patients with HCC (Llovet et al., 2008, 2015). Although they showed encouraging progress, there remains an urgent need to develop new therapies for HCC.

Fibroblast growth factor receptor 4 (FGFR4) is a receptor tyrosine kinase that selectively binds fibroblast growth factor 19 (FGF19) to activate a series of reactions, leading to bile formation, cell

**Abbreviations:** ABC, ATP-binding cassette; ANOVA, analysis of variance; AUC, area under plasma concentration-time curve; BCRP, breast cancer resistance protein; C<sub>brain</sub>, brain concentration; C<sub>max</sub>, maximum drug concentration in plasma; C<sub>testis</sub>, testis concentration; CNS, central nervous system; CYP, Cytochrome P450; *Cyp3a*<sup>-/-</sup>, *Cyp3a* knockout mice; *Cyp3aXAV*, *Cyp3a* knockout mice with specific expression of human CYP3A4 in liver and intestine; FGF19, fibroblast growth factor 19; FGFR4, fibroblast growth factor receptor 4; HCC, hepatocellular carcinoma; h (as prefix), human; LC-MS/MS, liquid chromatography coupled with tandem mass spectrometry; MDCK, Madin-Darby canine kidney; m (as prefix), mouse; OATP, organic anion transporting polypeptide; P<sub>brain</sub>, relative brain accumulation; P<sub>testis</sub>, relative testis accumulation; P-gp, P-glycoprotein; SD, standard deviation; SI, small intestinal tissue; SIC, small intestinal content; TKI, tyrosine kinase inhibitor; T<sub>max</sub>, time to reach maximum drug concentration in plasma

\* Corresponding author.

E-mail address: [a.schinkel@nki.nl](mailto:a.schinkel@nki.nl) (A.H. Schinkel).

<https://doi.org/10.1016/j.ijpharm.2019.118842>

Received 14 September 2019; Received in revised form 29 October 2019; Accepted 1 November 2019

Available online 20 November 2019

0378-5173/ © 2019 Elsevier B.V. All rights reserved.

differentiation and cell proliferation (Vainikka et al., 1994; Wu et al., 2011). Aberrant FGF19-FGFR4 complex formation has been identified as oncogenic in up to 32% of patients with HCC (Guichard et al., 2012). Moreover, FGF19/FGFR4 signaling contributes to the resistance of HCC to sorafenib (Gao et al., 2017). FGFR4 is therefore a promising target for the treatment of HCC harboring aberrant FGF19-FGFR4 signaling (Lu et al., 2019).

BLU9931 (Supplemental Fig. 1A), an exquisitely selective and potent ATP-competitive inhibitor of FGFR4, is efficacious in tumors with an intact FGFR4 signaling (Hagel et al., 2015). The discovery of BLU9931 led to the identification of a lead drug, fisogatinib (BLU-554; CS3008) (Supplemental Fig. 1B), with improved pharmaceutical properties which entered into clinical trial in 2015. Fisogatinib has shown significant antitumor activity, including complete and sustained tumor regression, in preclinical models of HCC (Kim et al., 2016). Moreover, an interim analysis of the Phase I study reports that fisogatinib is efficacious in FGF19 immunohistochemistry-positive HCC patients with an overall response rate (ORR) of 16% (95% CI, 6–31) and a disease control rate of 68%. This is much more promising than the currently-approved HCC treatments with response rates of 10% or less (Kim et al., 2016). The recommended dose of fisogatinib is 600 mg once daily, and it is generally well tolerated by patients (Kim et al., 2017). Fisogatinib is currently studied in a Phase I clinical trial (NCT02508467) for the treatment of HCC.

Drug pharmacokinetics can be influenced by certain efflux and influx transporters such as the ATP-binding cassette (ABC) transporters and the organic anion transporting polypeptides (OATPs) (Giacomini et al., 2010). ABCB1 (also known as multidrug resistance protein 1 (MDR1) or P-glycoprotein) and ABCG2 (also known as breast cancer resistance protein (BCRP)), two ABC transporters, are primarily expressed in the liver, intestinal epithelium and brain, as well as in a number of tumors (Borst and Elferink, 2002; Agarwal et al., 2011; Schinkel and Jonker, 2003). These transporters protect the body against harmful substances, and can also affect the therapeutic efficacy of drugs as they can limit the accumulation in organs like brain of tyrosine kinase inhibitors (TKIs) such as sorafenib and crizotinib, thus conferring therapy resistance to the tumor cells residing in this tissue (Li et al., 2018; Lagas et al., 2010; Tang et al., 2014). The incidence of brain metastases in HCC patients recently increased from approximately 1% to 2.2–7%, likely due to the recent progress in both early diagnosis using sensitive detection methods and better treatment with new targeted anti-cancer drugs, further emphasizing the importance to clarify whether fisogatinib interacts with these transporters (Wang et al., 2017).

OATP transporters are Na<sup>+</sup>-independent uptake transporters for endogenous and exogenous compounds like hormones, toxins, and numerous drugs (Kallikokoski and Niemi, 2009). OATP1A/1B proteins are of particular interest because of their high expression in the liver where they might affect oral availability and liver disposition of certain drugs (Iusuf et al., 2013). As the liver is the primary target tissue for fisogatinib, it is further important to investigate the possible interaction between fisogatinib and OATP1A/1B proteins.

Drug-metabolizing enzymes often work together with the drug transporters in modulating drug absorption, distribution, and elimination. Members of the Cytochrome P450 (CYP) superfamily of enzymes are responsible for most Phase I drug metabolism (Thelen and Dressman, 2009). Many drugs undergo metabolism by CYP3A4/5, the most abundant CYP3A enzymes in human liver and intestine, affecting their plasma exposure and even therapeutic efficacy by either inactivation or, sometimes, activation. Whether fisogatinib is significantly metabolized by CYP3A or not is currently unknown based on publicly available sources.

We aimed here to investigate whether or to what extent the oral availability and tissue distribution of fisogatinib are affected by ABCB1, ABCG2, OATP1A/1B, and CYP3A, using wild-type and appropriate genetically modified mouse models.

## 2. Material and methods

### 2.1. Chemicals

Fisogatinib (BLU-554; > 99%) was supplied by Carbosynth (Compton, Berkshire, UK). The inhibitors zosuquidar and Ko143 were acquired from Sequoia Research Products (Pangbourne, United Kingdom) and Tocris Bioscience (Bristol, United Kingdom), respectively. Bovine Serum Albumin (BSA) was obtained from Roche Diagnostics GmbH (Mannheim, Germany). Isoflurane was bought from Pharmachemie (Haarlem, The Netherlands) and Heparin (5000 IU ml<sup>-1</sup>) was purchased from Leo Pharma (Breda, The Netherlands). All other chemicals and reagents were obtained from Sigma-Aldrich (Steinheim, Germany).

### 2.2. Cell lines and transport assay

Polarized Madin-Darby Canine Kidney (MDCK-II) cells stably transduced with either human (h) ABCB1, hABCG2 or mouse (m) Abcg2 cDNA were used. These polarized epithelial cells show highly characteristic growth and active transport properties, including inhibitor sensitivity, confirming their proper identity, as also illustrated with some recently tested other compounds (e.g., Li et al., 2018). Cells were routinely tested negative for mycoplasma. The passage number when used in transport experiments was 10–15.

Transepithelial transport assays were performed on microporous polycarbonate membrane filters (3.0 µm pore size, 12 mm diameter, Transwell 3414, Corning, Kennebunk, ME). The parental MDCK-II cells and their variant subclones were seeded at a density of  $2.5 \times 10^5$  cells per well and cultured for 3 days to form an intact monolayer. Transepithelial electrical resistance was measured to confirm the integrity and permeability of the monolayer membrane before and after the transport phase.

The inhibitors zosuquidar (ABCB1 inhibitor) and/or Ko143 (ABCG2/Abcg2/inhibitor) were used at 5 µM, where appropriate, during the experiments after 1 h pre-incubation with these inhibitors in both compartments. The transport phase ( $t = 0$ ) was started by replacing the donor compartment medium with fresh Dulbecco's Modified Eagle Medium (DMEM) containing 10% (v/v) fetal bovine serum (FBS), 5 µM fisogatinib and an inhibitor if appropriate. The cells were kept in an environment of 37 °C in 5% CO<sub>2</sub> during the experiment. At the 1, 2, and 4 h time points, 50 µL aliquots were taken from the acceptor compartment and stored at –30 °C until they were measured by LC-MS/MS. Active transport of fisogatinib was defined using the transport ratio  $r$ , the amount of apically directed drug transport divided by basolaterally directed drug translocation after 4 h.

### 2.3. Animals

FVB mice were housed and handled according to institutional guidelines complying with Dutch and EU legislation. All experimental animal protocols were evaluated and approved by the institutional animal care and use committee. Male wild-type, *Abcb1a/1b*<sup>-/-</sup>, *Abcg2*<sup>-/-</sup>, *Abcb1a/1b;Abcg2*<sup>-/-</sup>, *Oatp1a/1b*<sup>-/-</sup>, *Cyp3a*<sup>-/-</sup> and *Cyp3aXAV* mice, all of a > 99% FVB genetic background, were used between 9 and 15 weeks of age with body weights in the range of 24.3–41.6 g (van de Steeg et al., 2010; van Herwaarden et al., 2007). As far as possible, experimental groups with similar average ages (and body weights) were used. The animals were kept in a temperature-controlled environment with a 12-hour light and 12-hour dark cycle and they received a standard diet (Transbreed, SDS Diets, Technilab-BMI, Someren, The Netherlands) and acidified water *ad libitum*.

### 2.4. Drug stock and working solution

For oral administration, fisogatinib was dissolved in dimethyl

sulfoxide (DMSO) to obtain a 50 mg/ml stock solution, which was stored at  $-30^{\circ}\text{C}$ . The dosing solutions (1 mg/ml) were prepared freshly on the day of experiment by diluting stock solution 2.5-fold with polysorbate 80/ethanol (1:1, v/v), and then 20-fold with a 10 mM hydrochloric acid solution ( $\text{pH} = 2$ ). The final concentrations for DMSO, polysorbate 80, ethanol, and 10 mM hydrochloric acid in the dosing solution were 2%, 1.5%, 1.5%, and 95% (v/v/v/v), respectively.

## 2.5. Plasma pharmacokinetics and organ accumulation of fisogatinib in mice

To minimize variation in absorption upon oral administration, mice were fasted for around 2–3 h before fisogatinib (10 mg/kg body weight) was administered by gavage into the stomach at 10  $\mu\text{L/g}$  body weight, using a blunt-ended needle. For the 1-h and 4-h experiment, serial tail vein blood sampling was performed at 3, 7.5, 15 and 30 min or 0.125, 0.25, 0.5, 1 and 2 h, respectively, using heparinized capillary tubes (Sarstedt, Germany). One or four hour after oral administration, isoflurane was used to anesthetize the mice and a final blood sample was obtained through cardiac puncture with a needle containing heparin as an anticoagulant. The blood samples were collected in Eppendorf tubes, followed by centrifugation at 9000g for 6 min at  $4^{\circ}\text{C}$  to isolate plasma. The plasma fraction was stored at  $-30^{\circ}\text{C}$  until analysis. Mice were sacrificed by cervical dislocation, after which the brain, liver, spleen, kidney, small intestinal tissue (SI), small intestinal content (SIC), and testis were quickly collected. The SI was rinsed with cold saline after the SIC was collected to remove any residual feces. The tissue homogenizations were performed by adding 1, 3, 1, 2, 3, 2 and 1 ml of 4% (w/v) bovine serum albumin to the weighed brain, liver, spleen, kidney, SI, SIC, and testis samples, respectively.

## 2.6. LC-MS/MS analysis

The concentrations of fisogatinib in cell culture medium, plasma samples and organ homogenates were determined using a sensitive and specific liquid chromatography-tandem mass spectrometry method as described (Dogan-Topal et al., 2019).

## 2.7. Pharmacokinetic calculations and statistical analysis

The pharmacokinetic parameters of fisogatinib were calculated by non-compartmental analysis methods using the PKSolver add-in program for Microsoft Excel. The area under the curve (AUC) was calculated with the trapezoidal rule without extrapolating to infinity. Parameters like the peak plasma concentration ( $C_{\text{max}}$ ) and time of peak plasma concentration ( $T_{\text{max}}$ ) were estimated from the original data. One-way analysis of variance (ANOVA) was used when multiple groups were compared and the Bonferroni *post hoc* correction was applied to accommodate multiple testing, using GraphPad Prism7 (GraphPad Software, La Jolla, CA). The two-sided unpaired student's *t* test was used when differences between two groups were compared. Differences were considered statistically significant when  $P < 0.05$ . All data are presented as geometric mean  $\pm$  SD.

## 3. Results

### 3.1. Fisogatinib is modestly transported by hABCB1 and slightly by mAbcg2 in vitro

Transepithelial drug transport was assessed using polarized monolayers of MDCK-II parental cells and its subclones overexpressing hABCB1, hABCG2 or mAbcg2. The parental cells showed no net transport of fisogatinib at 5  $\mu\text{M}$ , and transport was not affected by addition of the ABCB1 inhibitor zosuquidar ( $r = 0.99$ , Fig. 1A and B). In the cells overexpressing hABCB1, there was clear, albeit modest, apically directed transport of fisogatinib ( $r = 2.14$ , Fig. 1C), which was

inhibited by zosuquidar ( $r = 1.26$ , Fig. 1D).

In subsequent experiments with MDCK-II cells overexpressing hABCG2 and mAbcg2, zosuquidar was added to inhibit endogenous canine ABCB1 that may contribute to the transport of fisogatinib. mAbcg2-overexpressing MDCK-II cells slightly transported fisogatinib ( $r = 1.49$ , Fig. 1G) and transport was partly inhibited by the ABCG2 inhibitor Ko143 ( $r = 1.27$ , Fig. 1H). There was no detectable apically directed transport of fisogatinib in hABCG2-overexpressing cells (Fig. 1E and F). Fisogatinib thus appears to be modestly transported by hABCB1 and slightly by mAbcg2, but not detectably by hABCG2.

### 3.2. ABCB1 restricts fisogatinib brain and testis accumulation, but not plasma pharmacokinetics

To assess the possible effects of mAbcb1a/1b and mAbcg2 on the pharmacokinetics and tissue distribution of fisogatinib, we performed a 4 h pilot experiment in male wild-type and combination *Abcb1a/1b;Abcg2*<sup>-/-</sup> mice using an oral dose of 10 mg/kg fisogatinib. As shown in Supplemental Fig. 2 and Supplemental Table 1, fisogatinib was rapidly absorbed in both mouse strains, with the highest plasma concentrations observed in the same order as those obtained in humans. The plasma concentration-time curve ( $\text{AUC}_{0-4\text{h}}$ ) revealed no significant differences in fisogatinib oral availability between wild-type and *Abcb1a/1b;Abcg2*<sup>-/-</sup> mice.

Brain, liver, spleen, kidney, small intestinal tissue, and testis distribution of fisogatinib was also measured 4 h after oral administration. Substantial increases were observed in the brain concentration (7.6-fold), brain-to-plasma ratio (4.7-fold), and brain accumulation (6.5-fold) in *Abcb1a/1b;Abcg2*<sup>-/-</sup> mice compared to wild-type mice (Supplemental Fig. 3A–C; Supplemental Table 1). Qualitatively similar results were also observed for the testis (Supplemental Fig. 3D–F; Supplemental Table 1). In contrast, exposure of fisogatinib in other tested tissues only revealed at best small, albeit sometimes statistically significant, differences between the two strains when considering the tissue-to-plasma ratios (Supplemental Fig. 4).

Subsequently, a more extensive experiment was performed to further investigate the separate and combined roles of mAbcb1a/1b and mAbcg2 in oral availability and tissue distribution of fisogatinib. This experiment was terminated at 1 h, to ensure plasma levels were still comparatively high. We administered fisogatinib (10 mg/kg) orally to wild-type, *Abcb1a/1b*<sup>-/-</sup>, *Abcg2*<sup>-/-</sup>, and *Abcb1a/1b;Abcg2*<sup>-/-</sup> mice. As shown in Fig. 2A and Table 1, absorption was rapid in all strains, with a  $T_{\text{max}}$  around 15 min, but plasma exposure of fisogatinib ( $\text{AUC}_{0-1\text{h}}$ ) was not significantly different between the strains. Thus, mAbcb1a/1b and mAbcg2 had no marked impact on oral availability of fisogatinib at this dose. However, substantially higher brain concentrations were observed in *Abcb1a/1b*<sup>-/-</sup> (7.2-fold) and *Abcb1a/1b;Abcg2*<sup>-/-</sup> (9.2-fold) mice compared to wild-type mice, but not in single *Abcg2*<sup>-/-</sup> mice (Fig. 3A; Table 1). At 1 h, the brain-to-plasma ratios of fisogatinib were relatively low (0.12) in wild-type mice, and they were markedly increased by 5.2-fold and 7.0-fold in *Abcb1a/1b*<sup>-/-</sup> and *Abcb1a/1b;Abcg2*<sup>-/-</sup> mice, respectively (Fig. 3A and B; Table 1). Similar results were obtained for the brain accumulations (Fig. 3C). These data indicate that mAbcb1a/1b could profoundly restrict brain accumulation of fisogatinib, whereas mAbcg2 had little or no effect on this process.

As shown in Fig. 3D–F and Table 1, the testis-to-plasma ratios were substantially higher in *Abcb1a/1b*<sup>-/-</sup> (2.2-fold) and *Abcb1a/1b;Abcg2*<sup>-/-</sup> (2.9-fold) mice, but not in single *Abcg2*<sup>-/-</sup> mice relative to wild-type mice. The testis-to-plasma ratios were 0.55 in wild-type mice, which is around 4.6-fold higher than that for brain, indicating much higher intrinsic accessibility of testis for fisogatinib, and the relative impact of mAbcb1a/1b and mAbcg2 deficiency on testis accumulation was accordingly lower.

In contrast to brain and testis, the other tested organs including liver, spleen, kidney, and small intestinal tissue, did not demonstrate meaningful differences in tissue concentrations, tissue-to-plasma ratios

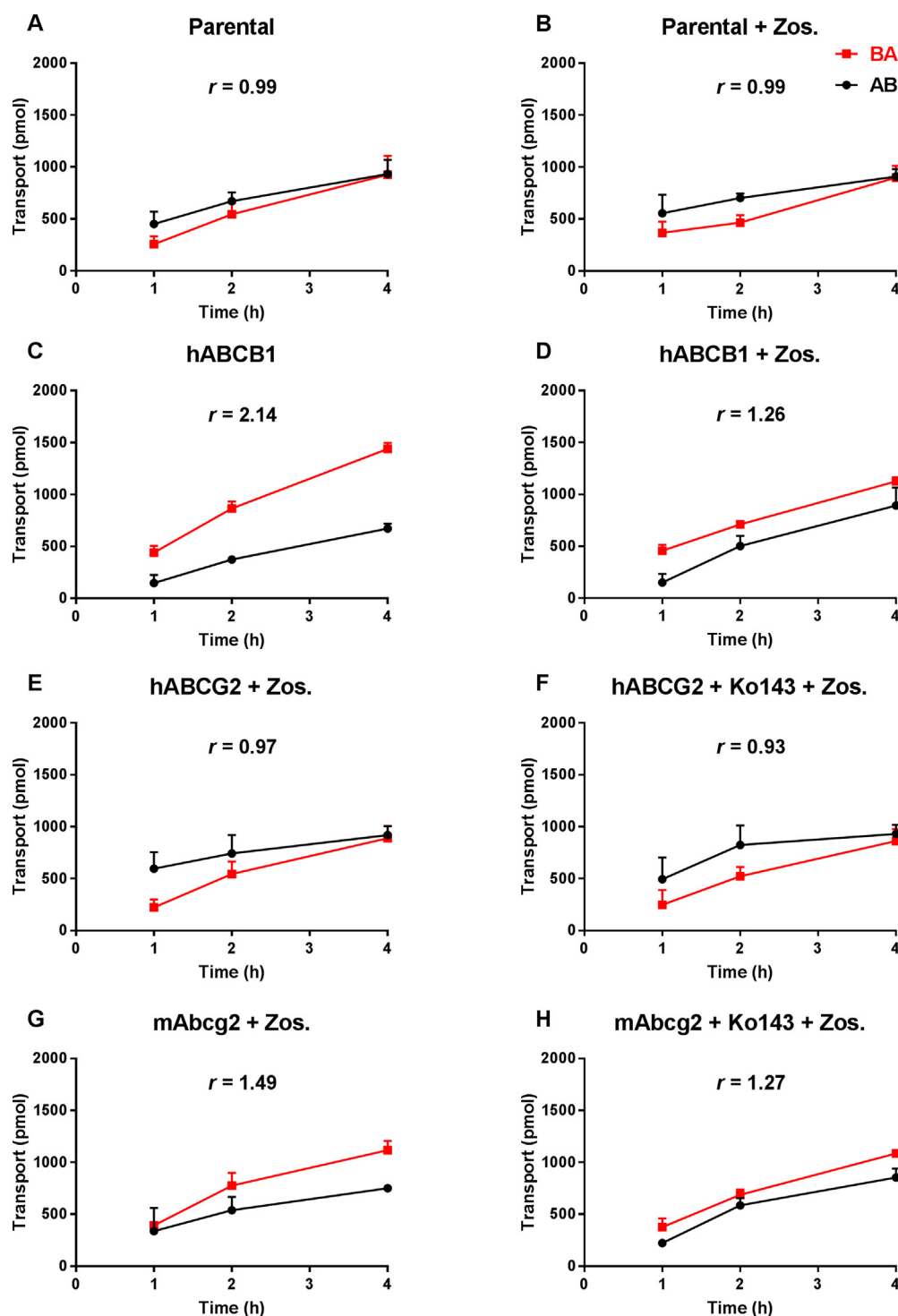


**Fig. 1.** Transepithelial transport of fisogatinib (5  $\mu$ M) assessed in MDCK-II cells either non-transduced (A, B), transduced with hABCB1 (C, D), hABCG2 (E, F) or mAbcg2 (G, H) cDNA. At  $t = 0$  h, fisogatinib was applied in the donor compartment and the concentrations in the acceptor compartment at  $t = 1, 2$ , and 4 h were measured and plotted as fisogatinib transport (pmol) in the graph ( $n = 3$ ). B, D–H: Zosuquidar (Zos., 5  $\mu$ M) was applied to inhibit human and/or endogenous canine ABCB1. F and H: the ABCG2 inhibitor Ko143 (5  $\mu$ M) was applied to inhibit ABCG2/Abcg2-mediated transport.  $r$ , relative transport ratio. BA (■), translocation from the basolateral to the apical compartment; AB (●), translocation from the apical to the basolateral compartment. Points, mean; bars, S.D.

or tissue accumulations of fisogatinib between mouse strains. The recovery of fisogatinib in small intestinal content was also not significantly different (Supplemental Fig. 5). Interestingly, the liver-to-plasma ratios of fisogatinib at 1 h were around 4, suggesting fisogatinib penetrates readily into this target tissue compared to other tissues, especially brain (0.12) and testis (0.55). This may be beneficial for fisogatinib as a treatment for hepatocellular carcinoma.

In spite of the markedly increased brain distribution of fisogatinib, we did not observe any spontaneous signs of acute toxicity of fisogatinib in the *Abcb1a/1b;Abcg2*<sup>-/-</sup> mice, unlike what we previously found for a few other tyrosine kinase inhibitors, including brigatinib (Li et al., 2018).

### 3.3. OATP1A/1B has little or no effect on plasma exposure and liver distribution of fisogatinib

While liver uptake is essential for the therapeutic use of fisogatinib, it is not clearly known how it enters the liver. OATPs can mediate liver uptake of drugs and thereby also affect their oral availability (Iusuf et al., 2013; van de Steeg et al., 2010). Very little is known about the possible interactions of fisogatinib with OATP/SLCO uptake transporters. We therefore performed a pilot experiment administering fisogatinib (10 mg/kg) to male wild-type and *Oatp1a/1b*<sup>-/-</sup> mice, and analyzed the plasma concentrations up to 4 h and liver-to-plasma ratios at 4 h. The fisogatinib plasma AUC<sub>0-4h</sub> was not significantly different



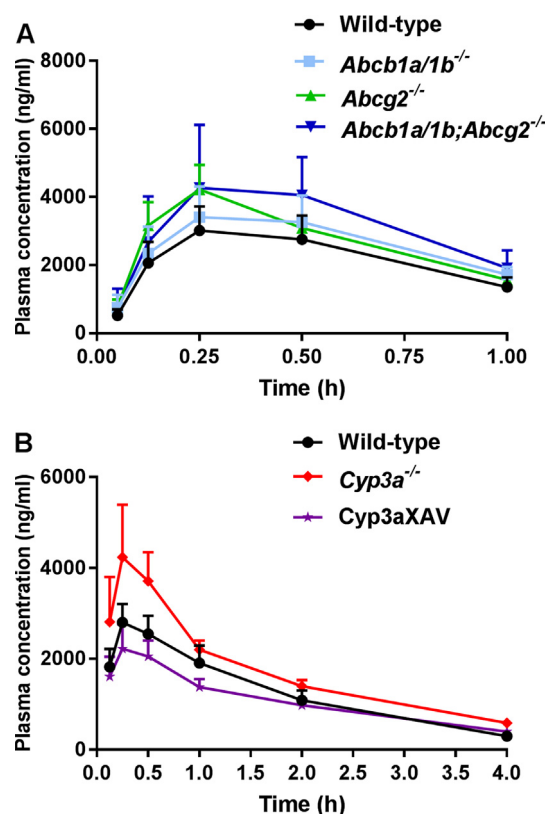


**Fig. 2.** Plasma concentration-time curves of fisogatinib in male mice. Panel A: wild-type, *Abcb1a/1b*<sup>-/-</sup>, *Abcg2*<sup>-/-</sup>, and *Abcb1a/1b;Abcg2*<sup>-/-</sup> mice over 1 h after oral administration of 10 mg/kg fisogatinib (n = 6). Panel B: wild-type, *Cyp3a*<sup>-/-</sup> and *Cyp3aXAV* mice over 4 h after oral administration of 10 mg/kg fisogatinib (n = 6–7).

between wild-type and *Oatp1a/1b*<sup>-/-</sup> mice (Supplemental Fig. 2; Supplemental Table 1). However, there was a borderline significantly lower (0.83-fold, *P* = 0.02, Supplemental Fig. 4) liver-to-plasma ratio observed in *Oatp1a/1b*<sup>-/-</sup> mice. To further investigate a possible effect of *Oatp1a/1b* on oral availability and liver distribution of fisogatinib, a follow-up experiment was terminated at 1 h at relatively high plasma concentrations. No statistically significant differences were observed either in plasma exposure (*AUC*<sub>0-1h</sub>) or liver-to-plasma ratios (Fig. 4;

Table 1). This indicates that *Oatp1a/1b* proteins have little, if any, impact on fisogatinib oral availability or liver distribution in mice.

### 3.4. CYP3A substantially restricts oral availability of fisogatinib

Many drugs are metabolized by CYP3A, leading to inactivation (or sometimes activation), causing low plasma exposure of the parent drug. This often affects its therapeutic efficacy and/or toxicity. To assess the impact of CYP3A on fisogatinib pharmacokinetics, we used male wild-type, *Cyp3a* knockout (*Cyp3a*<sup>-/-</sup>), and *Cyp3a*<sup>-/-</sup> mice with specific transgenic expression of human CYP3A4 in liver and intestine (*Cyp3aXAV*) mice in a 4 h experiment. After oral administration of 10 mg/kg fisogatinib, blood and organs were collected. As shown in Fig. 2B and Supplemental Table 1, fisogatinib absorption was again rapid, with the time to reach peak plasma concentrations at around 15 min in each strain. The oral *AUC*<sub>0-4h</sub> in *Cyp3a*<sup>-/-</sup> mice was 1.4-fold higher (*P* < 0.01) than that in wild-type mice, whereas plasma exposure in *Cyp3aXAV* mice was substantially decreased by 1.6-fold (*P* < 0.001) relative to *Cyp3a*<sup>-/-</sup> mice (Fig. 2B; Supplemental Table 1). This indicates that human CYP3A4 can play a substantial role in fisogatinib metabolism and oral availability.

In contrast to the overall plasma exposure, the relative tissue disposition of fisogatinib as judged by tissue accumulation showed few meaningful differences between wild-type, *Cyp3a*<sup>-/-</sup> and *Cyp3aXAV* mice (Supplemental Figs. 3 and 4; Supplemental Table 1). Modest but sometimes statistically significant decreases observed in tissue-to-plasma ratios, especially in testis, may in part have to do with a comparatively high plasma concentration at 4 h relative to the overall plasma exposure in the *Cyp3a*<sup>-/-</sup> and *Cyp3aXAV* mice compared to wild-type mice (Fig. 2B). Collectively, our results indicate that fisogatinib is substantially metabolized by mouse *Cyp3a* and human CYP3A4, which affects the oral availability of fisogatinib.

## 4. Discussion

We found that the novel FGFR4 inhibitor fisogatinib is modestly transported *in vitro* by human ABCB1 and slightly by mouse *Abcg2*, but not detectably by human ABCG2. Upon oral administration of 10 mg/kg fisogatinib, *mAbcb1a/1b* and *mAbcg2* had no detectable impact on restricting oral availability of fisogatinib. However, the brain accumulation substantially increased by 6.3-fold and 7.2-fold in *Abcb1a/1b*<sup>-/-</sup> and *Abcb1a/1b;Abcg2*<sup>-/-</sup> mice, respectively, but not in single *Abcg2*<sup>-/-</sup> mice. Qualitatively similar results were observed for testis

**Table 1**

Plasma, brain, testis, and liver pharmacokinetic parameters of fisogatinib 1 h after oral administration of 10 mg/kg fisogatinib to male wild-type, *Abcb1a/1b*<sup>-/-</sup>, *Abcg2*<sup>-/-</sup>, *Abcb1a/1b;Abcg2*<sup>-/-</sup>, and *Oatp1a/1b*<sup>-/-</sup> mice.

Parameter	Genotype				
	Wild-type	<i>Abcb1a/1b</i> <sup>-/-</sup>	<i>Abcg2</i> <sup>-/-</sup>	<i>Abcb1a/1b;Abcg2</i> <sup>-/-</sup>	<i>Oatp1a/1b</i> <sup>-/-</sup>
<i>AUC</i> <sub>0-1h</sub> , ng/ml.h	2179 ± 454	2576 ± 517	2710 ± 302	3116 ± 919	2482 ± 391
Fold change <i>AUC</i> <sub>0-1h</sub>	1.00	1.18	1.24	1.43	1.14
<i>C</i> <sub>max</sub> , ng/ml	3018 ± 709	3489 ± 846	4225 ± 722	4480 ± 1508	3407 ± 596
<i>T</i> <sub>max</sub> , h	0.25–0.5	0.25–0.5	0.25–0.5	0.25–0.5	0.25–0.5
<i>C</i> <sub>brain</sub> , ng/g	165 ± 49	1184 ± 87***	205 ± 20	1514 ± 153***(^)	186 ± 73
Fold increase <i>C</i> <sub>brain</sub>	1.0	7.2	1.2	9.2	1.1
Brain-to-plasma ratio	0.12 ± 0.017	0.70 ± 0.01***	0.13 ± 0.01	0.83 ± 0.17***	0.11 ± 0.04
Fold change ratio	1.0	5.2	1.1	7.0	0.93
<i>C</i> <sub>testis</sub> , ng/g	740 ± 180	2112 ± 378***	752 ± 115	2885 ± 371***(^)	814 ± 117
Fold increase <i>C</i> <sub>testis</sub>	1.0	2.9	1.0	3.9	1.1
Testis-to-plasma ratio	0.55 ± 0.10	1.2 ± 0.13***	0.49 ± 0.13	1.6 ± 0.47***	0.49 ± 0.06
Fold change ratio	1.0	2.2	0.89	2.9	0.90
Liver-to-plasma ratio	4.12 ± 0.57	3.63 ± 0.57	3.92 ± 0.32	4.50 ± 1.09	3.91 ± 0.45
Fold change ratio	1.0	0.88	0.95	1.1	0.95

*AUC*<sub>0-1h</sub>, area under the plasma concentration–time curve; *C*<sub>max</sub>, maximum concentration in plasma; *T*<sub>max</sub>, time range (h) of maximum plasma concentration; *C*<sub>tissue</sub>, tissue concentration. Data are given as mean ± S.D. (n = 6). \*, *P* < 0.05; \*\*, *P* < 0.01; \*\*\*, *P* < 0.001 compared to wild-type mice. ^, *P* < 0.05; ~, *P* < 0.01; ~~, *P* < 0.001 comparing *Abcb1a/1b;Abcg2*<sup>-/-</sup> to *Abcb1a/1b*<sup>-/-</sup> mice.

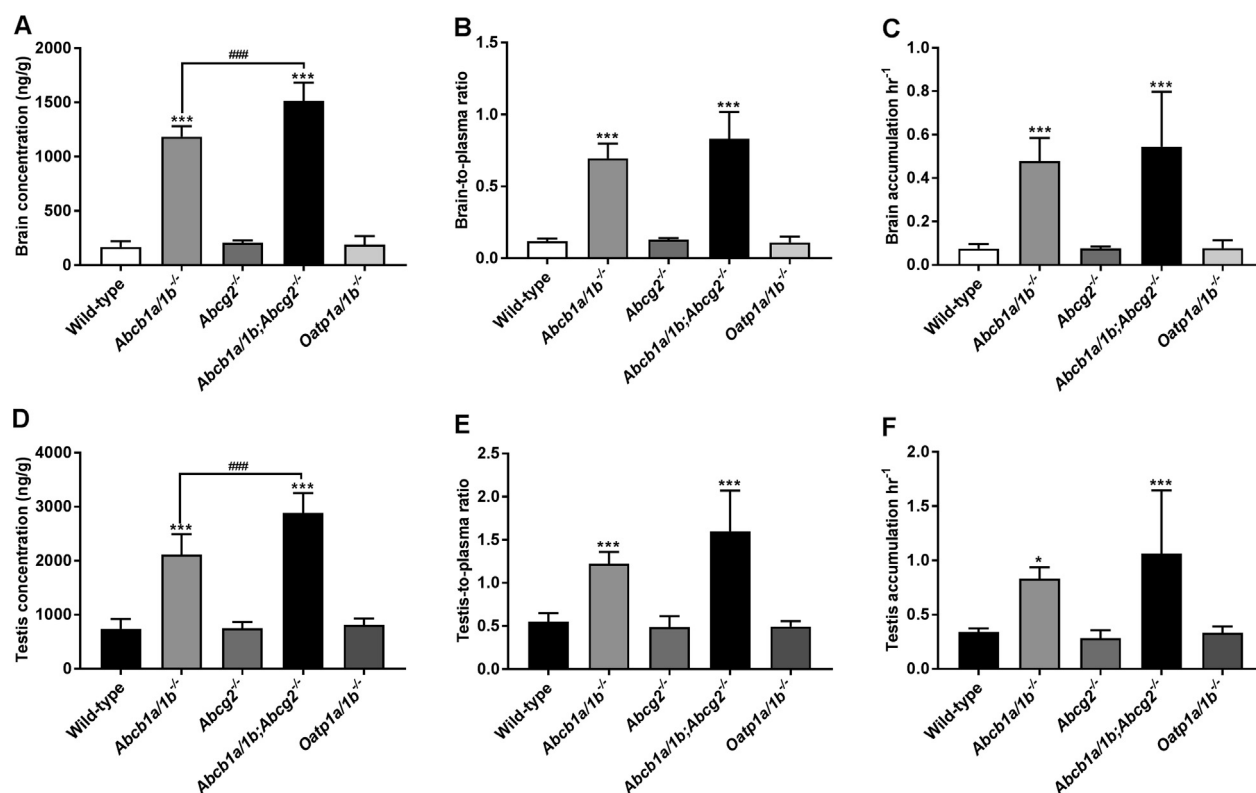


**Fig. 3.** Brain or testis concentration (A, D), brain- or testis-to-plasma ratio (B, E), and brain or testis accumulation (C, F) of fisogatinib in male wild-type, *Abcb1a/1b*<sup>-/-</sup>, *Abcg2*<sup>-/-</sup>, *Abcb1a/1b;Abcg2*<sup>-/-</sup>, and *Oatp1a/1b*<sup>-/-</sup> mice 1 h after oral administration of 10 mg/kg fisogatinib. Data are presented as mean  $\pm$  S.D. (n = 6). \*,  $P < 0.05$ ; \*\*,  $P < 0.01$ ; \*\*\*,  $P < 0.001$  compared to wild-type mice and #,  $P < 0.05$ ; ##,  $P < 0.01$ ; ###,  $P < 0.001$  comparing *Abcb1a/1b;Abcg2*<sup>-/-</sup> to *Abcb1a/1b*<sup>-/-</sup> mice.

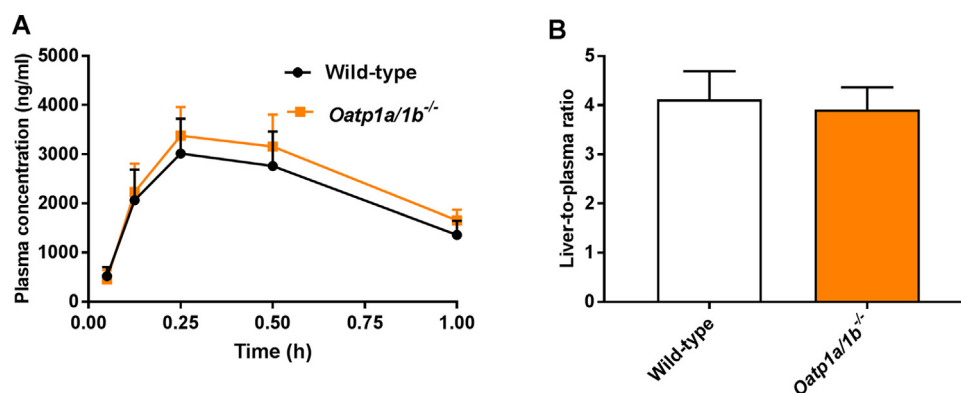


**Fig. 4.** Plasma concentration-time curves (panel A) and liver-to-plasma ratio (panel B) of fisogatinib in male wild-type and *Oatp1a/1b*<sup>-/-</sup> mice over 1 h after oral administration of 10 mg/kg fisogatinib (n = 6).

accumulation. In contrast, fisogatinib distribution to other tissues was not markedly changed due to the transporter deficiencies. The ABCB1 P-glycoprotein in the mouse BBB and BTB thus actively keeps fisogatinib out of the brain and testis. We further found that *Oatp1a/1b* deficiency did not markedly alter oral fisogatinib liver distribution and plasma pharmacokinetics. However, fisogatinib oral availability in mice was clearly limited by mouse *Cyp3a* and even more so by transgenic human *CYP3A4*, suggesting that *CYP3A* can play a substantial role in metabolic clearance of fisogatinib.

To date, potent and selective FGFR4 inhibitors are not available to patients. The lack of kinase selectivity of candidate FGFR4 inhibitors often results in toxicity related to off-target activity, whereas inhibition of FGFR1 and FGFR3 causes soft-tissue mineralization and hyperphosphatemia (Degirolamo et al., 2016). Fisogatinib demonstrates exquisite kinase selectivity, targeting FGFR4 while sparing all other

FGFR paralogs. A Phase I clinical trial showed that fisogatinib provides acceptable tolerability with mostly 1 or 2 adverse effects (Kim et al., 2017). This manageable on-target toxicity reported by the manufacturer might be a consequence of the FGFR4 selectivity of fisogatinib. Moreover, no noticeable signs of acute toxicity of fisogatinib were observed in the current mouse study.

While fisogatinib was modestly transported by hABCB1 and slightly by mAbcg2 *in vitro*, the brain accumulation of fisogatinib was only substantially restricted by mAbcb1a/1b, but not by mAbcg2. The expression level of *Abcb1a* protein is approximately 3- to 4-fold higher compared to *Abcg2* at the mouse BBB, further explaining the lack of functional impact of *Abcg2* (Kamiie et al., 2008). In contrast, for sorafenib and regorafenib, two currently registered TKIs for HCC, the brain distribution is limited by both *Abcb1a/1b* and *Abcg2*, with *Abcg2* playing a dominant role (Lagas et al., 2010; Kort et al., 2015).

In this study, we observed a clear impact of context-dependency in ABC transporter activity. The absence of Abcb1a/1b does not affect oral availability, but does influence brain accumulation. The unchanged oral absorption of fisogatinib suggests that there are high-capacity uptake systems for fisogatinib in the intestinal epithelium of mice. While the identity of these putative transport systems is as yet unknown, the gut has evolved to absorb a large variety of nutrients, so there may be several candidates. The resulting high intestinal influx of fisogatinib initially likely overwhelms the efflux activity of Abcb1a/1b, explaining why we see little or no impact of Abcb1a/1b deficiency on the oral availability. In contrast to the gut epithelium, the BBB is highly selective, and generally allows only the mediated uptake of specific nutrients and signaling molecules essential for brain function. The low brain penetration of fisogatinib suggests that any intestinal-type uptake systems for fisogatinib are absent from the BBB, or only lowly expressed. The low overall uptake rate of fisogatinib across the BBB makes it far easier for Abcb1a/1b in the BBB to effectively counteract this influx. Furthermore, the fisogatinib blood concentrations to which the BBB is exposed are likely far lower than the intestinal luminal concentration of fisogatinib shortly after oral administration. It could thus be that intestinal Abcb1a/1b is then completely saturated, whereas BBB Abcb1a/1b is not.

HCC is able to metastasize to the brain and the incidence of brain metastasis in HCC has been reported to increase to 2.0–7.7%, which is probably the result of recent progress in both early diagnosis using sensitive detection methods and better treatment with new targeted anti-cancer drugs (Tang et al., 2014). It is therefore of importance that newly developed anti-HCC drugs can easily penetrate into the brain, either by themselves or through modulation of any relevant transporters in the BBB. While we found a relatively poor brain penetration of fisogatinib in wild-type mice, with a brain-to-plasma ratio of about 0.12, this penetration could be enhanced by up to 7-fold by removing P-glycoprotein in the BBB. This P-glycoprotein function may be of relevance for limiting therapeutic efficacy against brain metastases in HCC, in case P-glycoprotein in the human brain has a similar impact as in the mouse brain. If so, looking ahead for a broader clinical use of fisogatinib, we could also use this insight to improve (boost) brain concentration of fisogatinib using pharmacological inhibitors of P-glycoprotein, such as elacridar. Even though this principle has been found to be feasible in mouse models for some other drugs (Li et al., 2018a, 2018b, 2019), any attempt to apply an efficacious ABCB1/ABCG2 inhibitor in patients in order to improve the CNS distribution of fisogatinib should be very carefully monitored. For instance, we previously observed some severe and lethal toxicity of the oral ALK/EGFR inhibitor brigatinib in mice with genetic knockout or pharmacological inhibition of mAbcb1a/1b and mAbcg2 (Li et al., 2018).

Compared to other tested tissues, fisogatinib showed relatively good penetration into the liver with liver-to-plasma ratios of around 4 in wild-type mice. The liver represents the main therapeutic target tissue for fisogatinib, so it is useful for fisogatinib to have good liver penetration in order to treat HCC. The substantial hepatic uptake of fisogatinib may be related to passive diffusion and/or presence of relevant uptake transporters, but it is unlikely that OATP1A/1B transporters play a significant role here, as we did not observe any significant differences in either plasma exposure or liver distribution between wild-type and *Oatp1a/1b*<sup>-/-</sup> mice.

There is very little information publicly available on the possible interaction between fisogatinib and CYP3A. We found that both mouse Cyp3a and especially human CYP3A4 can markedly reduce the oral availability and thus overall systemic exposure of fisogatinib, while the relative tissue distribution of the drug was not much affected. This suggests that the body exposure and metabolic clearance of fisogatinib would likely be noticeably affected by variable CYP3A activity in patients, due to either drug-drug interactions or genetic polymorphisms. Our data indicate a clear, albeit modest, *in vivo* interaction of fisogatinib and CYP3A. This probably will need to be considered in clinical dosing

of fisogatinib. Moreover, CYP3A is highly expressed in the liver, which therefore represents not only the therapeutic target tissue, but potentially also one of the main metabolic tissues for fisogatinib. This further emphasizes the importance to critically monitor when administering fisogatinib with CYP3A inducers and/or inhibitors.

## 5. Conclusions

To the best of our knowledge, this is the first study documenting that fisogatinib is markedly transported by ABCB1 and slightly by mABCG2 *in vitro* and that in mice its brain accumulation, but not oral availability, is primarily restricted by ABCB1 P-glycoprotein. Oral pharmacokinetics and liver distribution of fisogatinib were not much affected by *Oatp1a/1b* deficiency. Furthermore, human CYP3A4 and mouse CYP3A can substantially limit the systemic exposure of fisogatinib, without altering its relative tissue distribution. While the findings in this study will obviously need to be tested in their own right for their validity in patients, we expect that they may be used to further enhance the therapeutic application and efficacy of fisogatinib, perhaps especially against brain metastases in HCC.

## Declaration of Competing Interest

The authors declare the following financial interests/personal relationships which may be considered as potential competing interests: The research group of Alfred H. Schinkel receives revenue from commercial distribution of some of the mouse strains used in this study. The other authors declare no conflict of interest.

## Acknowledgements

We gratefully acknowledge Dr. B. Dogan-Topal (Ankara University, Faculty of Pharmacy, Department of Analytical Chemistry, Ankara, Turkey) for the collaboration on the development of the fisogatinib (BLU-554) LC-MS/MS assay.

## Funding

This work was funded in part by the China Scholarship Council (CSC Scholarship No. 201606220081 to W. Li).

## Authors' contributions

WL, ME, and AS designed the study, analyzed the data and wrote the manuscript. WL, ME, RS, and YW performed the experimental parts of the study. ML contributed reagents, materials, and mice. JB and RS supervised the bioanalytical part of the studies and checked the content and language of manuscript. All authors read and approved the final manuscript.

## Availability of data and materials

The datasets used and/or analyzed during the current study are included in this article or are available from the corresponding author on reasonable request.

## Appendix A. Supplementary data

Supplementary data to this article can be found online at <https://doi.org/10.1016/j.ijpharm.2019.118842>.

## References

- Agarwal, S., Hartz, A.M., Elmquist, W.F., Bauer, B., 2011. Breast cancer resistance protein and P-glycoprotein in brain cancer: two gatekeepers team up. *Curr. Pharm. Des.* 17 (26), 2793–2802.

- Balogh, J., Victor 3rd, D., Asham, E.H., Burroughs, S.G., Boktour, M., Saharia, A., et al., 2016. Hepatocellular carcinoma: a review. *J. Hepatocell Carcinoma*. 3, 41–53.
- Borst, P., Elferink, R.O., 2002. Mammalian ABC transporters in health and disease. *Annu. Rev. Biochem.* 71, 537–592.
- Bray, F., Ferlay, J., Soerjomataram, I., Siegel, R.L., Torre, L.A., Jemal, A., 2018. Global cancer statistics 2018: GLOBOCAN estimates of incidence and mortality worldwide for 36 cancers in 185 countries. *CA Cancer J. Clin.* 68 (6), 394–424.
- Degriolamo, C., Sabba, C., Moschetta, A., 2016. Therapeutic potential of the endocrine fibroblast growth factors FGF19, FGF21 and FGF23. *Nat. Rev. Drug Discovery* 15 (1), 51–69.
- Dogan-Topal, B., Li, W., Schinkel, A.H., Beijnen, J.H., Sparidans, R.W., 2019. Quantification of FGFR4 inhibitor BLU-554 in mouse plasma and tissue homogenates using liquid chromatography-tandem mass spectrometry. *J. Chromatogr., B: Anal. Technol. Biomed. Life Sci.* 1110–1111, 116–123.
- Gao, L., Wang, X., Tang, Y., Huang, S., Hu, C.A., Teng, Y., 2017. FGF19/FGFR4 signaling contributes to the resistance of hepatocellular carcinoma to sorafenib. *J. Exp. Clin. Cancer Res.* CR 36 (1), 8.
- Giacomini, K.M., Huang, S.M., Tweedie, D.J., Benet, L.Z., Brouwer, K.L., Chu, X., et al., 2010. Membrane transporters in drug development. *Nat. Rev. Drug Discovery* 9 (3), 215–236.
- Guichard, C., Amadio, G., Imbeaud, S., Ladeiro, Y., Pelletier, L., Maad, I.B., et al., 2012. Integrated analysis of somatic mutations and focal copy-number changes identifies key genes and pathways in hepatocellular carcinoma. *Nat. Genet.* 44 (6), 694–698.
- Hagel, M., Miduturu, C., Sheets, M., Rubin, N., Weng, W., Stransky, N., et al., 2015. First selective small molecule inhibitor of FGFR4 for the treatment of hepatocellular carcinomas with an activated FGFR4 signaling pathway. *Cancer Discov.* 5 (4), 424–437.
- Iusuf, D., van Esch, A., Hobbs, M., Taylor, M., Kenworthy, K.E., van de Steeg, E., et al., 2013. Murine Oatp1a/1b uptake transporters control rosuvastatin systemic exposure without affecting its apparent liver exposure. *Mol. Pharmacol.* 83 (5), 919–929.
- Kalliokoski, A., Niemi, M., 2009. Impact of OATP transporters on pharmacokinetics. *Br. J. Pharmacol.* 158 (3), 693–705.
- Kamiie, J., Ohtsuki, S., Iwase, R., Ohmine, K., Katsukura, Y., Yanai, K., et al., 2008. Quantitative atlas of membrane transporter proteins: development and application of a highly sensitive simultaneous LC/MS/MS method combined with novel in-silico peptide selection criteria. *Pharm. Res.* 25 (6), 1469–1483.
- Kim, R., Sharma, S., Meyer, T., Sarker, D., Macarulla, T., Sung, M., et al., 2016. First-in-human study of BLU-554, a potent, highly-selective FGFR4 inhibitor designed for hepatocellular carcinoma (HCC) with FGFR4 pathway activation. *Eur. J. Cancer* 69, S41.
- Kim, R., Sarker, D., Macarulla, T., Yau, T., Choo, S.P., Meyer, T., et al., 2017. 3650Phase 1 safety and clinical activity of BLU-554 in advanced hepatocellular carcinoma (HCC). *Annals of Oncology*. 28 (suppl.5).
- Kort, A., Durmus, S., Sparidans, R.W., Wagenaar, E., Beijnen, J.H., Schinkel, A.H., 2015. Brain and testis accumulation of regorafenib is restricted by breast cancer resistance protein (BCRP/ABCG2) and P-glycoprotein (P-GP/ABCB1). *Pharm. Res.* 32 (7), 2205–2216.
- Lagas, J.S., van Waterschoot, R.A., Sparidans, R.W., Wagenaar, E., Beijnen, J.H., Schinkel, A.H., 2010. Breast cancer resistance protein and P-glycoprotein limit sorafenib brain accumulation. *Mol. Cancer Ther.* 9 (2), 319–326.
- Li, W., Sparidans, R.W., Wang, Y., Lebre, M.C., Wagenaar, E., Beijnen, J.H., et al., 2018. P-glycoprotein (MDR1/ABCB1) restricts brain accumulation and cytochrome P450–3A (CYP3A) limits oral availability of the novel ALK/ROS1 inhibitor lorlatinib. *Int. J. Cancer* 143 (8), 2029–2038.
- Li, W., Sparidans, R.W., Wang, Y., Lebre, M.C., Beijnen, J.H., Schinkel, A.H., 2018. P-glycoprotein and breast cancer resistance protein restrict brigatinib brain accumulation and toxicity, and alongside CYP3A, limit its oral availability. *Pharmacol. Res.* 137, 47–55.
- Li, W., Tibben, M., Wang, Y., Lebre, M.C., Rosing, H., Beijnen, J.H., et al., 2019. P-glycoprotein (MDR1/ABCB1) controls brain accumulation and intestinal disposition of the novel TGF-beta signaling pathway inhibitor galunisertib. *Int. J. Cancer*.
- Llovet, J.M., Ricci, S., Mazzaferro, V., Hilgard, P., Gane, E., Blanc, J.F., et al., 2008. Sorafenib in advanced hepatocellular carcinoma. *New Engl. J. Med.* 359 (4), 378–390.
- Llovet, J.M., Villanueva, A., Lachenmayer, A., Finn, R.S., 2015. Advances in targeted therapies for hepatocellular carcinoma in the genomic era. *Nat. Rev. Clin. Oncol.* 12 (8), 436.
- Lu, X., Chen, H., Patterson, A.V., Smail, J.B., Ding, K., 2019. Fibroblast growth factor receptor 4 (FGFR4) selective inhibitors as hepatocellular carcinoma therapy: advances and prospects. *J. Med. Chem.* 62 (6), 2905–2915.
- Schinkel, A.H., Jonker, J.W., 2003. Mammalian drug efflux transporters of the ATP binding cassette (ABC) family: an overview. *Adv. Drug Deliv. Rev.* 55 (1), 3–29.
- Tang, S.C., Nguyen, L.N., Sparidans, R.W., Wagenaar, E., Beijnen, J.H., Schinkel, A.H., 2014. Increased oral availability and brain accumulation of the ALK inhibitor crizotinib by coadministration of the P-glycoprotein (ABCB1) and breast cancer resistance protein (ABCG2) inhibitor elacridar. *Int. J. Cancer* 134 (6), 1484–1494.
- Thelen, K., Dressman, J.B., 2009. Cytochrome P450-mediated metabolism in the human gut wall. *J. Pharm. Pharmacol.* 61 (5), 541–558.
- Vainikka, S., Joukov, V., Wennstrom, S., Bergman, M., Pelicci, P.G., Alitalo, K., 1994. Signal transduction by fibroblast growth factor receptor-4 (FGFR-4). Comparison with FGFR-1. *J. Biol. Chem.* 269 (28), 18320–18326.
- van de Steeg, E., Wagenaar, E., van der Kruijsen, C.M., Burggraaff, J.E., de Waart, D.R., Elferink, R.P., et al., 2010. Organic anion transporting polypeptide 1a/1b-knockout mice provide insights into hepatic handling of bilirubin, bile acids, and drugs. *J. Clin. Invest.* 120 (8), 2942–2952.
- van Herwaarden, A.E., Wagenaar, E., van der Kruijsen, C.M., van Waterschoot, R.A., Smit, J.W., Song, J.Y., et al., 2007. Knockout of cytochrome P450 3A yields new mouse models for understanding xenobiotic metabolism. *J. Clin. Invest.* 117 (11), 3583–3592.
- Wang, S., Wang, A., Lin, J., Xie, Y., Wu, L., Huang, H., et al., 2017. Brain metastases from hepatocellular carcinoma: recent advances and future avenues. *Oncotarget*. 8 (15), 25814–25829.
- Wu, A.L., Coulter, S., Liddle, C., Wong, A., Eastham-Anderson, J., French, D.M., et al., 2011. FGF19 regulates cell proliferation, glucose and bile acid metabolism via FGFR4-dependent and independent pathways. *PLoS ONE* 6 (3), e17868.